J Mol Model (2008) 14:717–726
DOI 10.1007/s00894-008-0284-1

ORIGINAL PAPER

The molecular structure of a curl-shaped retinal isomer

Robert Send · Dage Sundholm

Received: 2 November 2007 / Accepted: 5 February 2008 / Published online: 20 March 2008

Abstract Computational studies of retinal protonated Schiff base (PSB) isomers show that a twisted curl-shaped conformation of the retinyl chain is a new low-lying minimum on the ground-state potential energy surface. The curl-shaped isomer has a twisted structure in the vicinity of the C_{11}=C_{12} double bond where the 11-*cis* retinal PSB isomerizes in the rhodopsin photoreaction. The twisted configuration is a trapped structure between the 11-*cis* and all-*trans* isomers. Rotation around the C_{10}–C_{11} single bond towards the 11-*cis* structure is prevented by steric interactions of the two methyl groups on the retinyl chain and by the torsion barrier of the C_{10}–C_{11} bond in the other direction. Calculations of spectroscopic properties of the 11-*cis*, all-*trans*, and curl-shaped isomers provide useful data for future identification of the new retinal PSB isomer. Circular dichroism (CD) spectroscopy might be used to distinguish between the retinal PSB isomers. The potential energy surface for the orientation of the β-ionone ring of the 11-*cis* retinal PSB reveals three minima depending on the torsion angle of the β-ionone ring. Two of the minima correspond to 6-s-*cis* configurations and one has the β-ionone ring in 6-s-*trans* position. The calculated CD spectra for the two 6-s-*cis* configurations differ significantly indicating that the sign of the β-ionone ring torsion angle could be determined using CD spectroscopy. Calculations of the CD spectra suggest that a flip of the β-ionone ring might occur during the first 1 ps of the photoreaction. Rhodopsin has a negative torsion angle for the β-ionone ring, whereas the change in the sign of the first peak in the experimental CD spectrum for bathorhodopsin could suggest that it has a positive torsion angle for the β-ionone ring. Calculated nuclear magnetic resonance (NMR) shielding constants and infrared (IR) spectra are also reported for the retinal PSB isomers.

Keywords Circular dichroism · Density functional theory · Retinal · Rhodopsin · Time-dependent density functional theory

Electronic supplementary material The online version of this article (doi:10.1007/s00894-008-0284-1) contains supplementary material, which is available to authorized users.

R. Send
Institut für Physikalische Chemie, Universität Karlsruhe,
Kaiserstrasse 12,
D-76128 Karlsruhe, Germany

D. Sundholm (✉)
Department of Chemistry, University of Helsinki,
P.O. Box 55, (A.I. Virtanens plats 1),
FIN-00014 Helsinki, Finland
e-mail: sundholm@chem.helsinki.fi

Introduction

The 11-*cis*-retinal protonated Schiff base (PSB) chromophore is the photoreceptor in rhodopsin responsible for the twilight vision of the rod visual cells. The absorption of a photon triggers a complex photoreaction involving several intermediates. Low-temperature time-resolved spectroscopy measurements showed that the first species formed in the reaction is photorhodopsin [1–3]. It is created within 200 fs after the photoexcitation and is a precursor to bathorhodopsin [4–6]. The molecular structure of photorhodopsin is largely unresolved because it decays spontaneously into bathorhodopsin which is the first intermediate that can be trapped and characterized at low temperatures [7–9]. It was proposed already in 1963 that bathorhodopsin has a twisted all-*trans* structure [10]. The *trans* conformation of the C_{11}=C_{12} double bond was definitively settled by the recent X-ray study of illuminated rhodopsin crystals [8]. Femto-

second-stimulated Raman spectroscopy (FSRS) studies by Mathies et al. also suggested that bathorhodopsin has a twisted *trans* conformation with a torsion angle of −144° about the C_{11}=C_{12} double bond [6].

A recent computational study of the molecular structure of the first excited state of the 11-*cis* retinal PSB yielded a strongly twisted molecular structure with the hydrogens at C_{10} and C_{11} in perpendicular orientation [11]. The numbering of the carbon atoms is shown in Fig. 1. The torsional twist of the C_{10}–C_{11} bond led to a tiny gap between the highest-occupied molecular orbital (HOMO) and the lowest-unoccupied molecular orbital (LUMO). The small HOMO-LUMO gap indicates that the structure is approaching a conical intersection. To follow the wave packet on the other side of the conical intersection, the structure obtained in the excited-state optimization was used as the starting point for the ground-state optimization in this work. Thus, for the last geometry in the excited-state optimization for which we were able to solve the Kohn-Sham equations, we switched from optimization on the potential energy surface of the excited state to the ground-state. The ground-state structural optimization yielded surprisingly a new curl-shaped retinal PSB isomer with a strongly twisted retinyl chain. The carbon backbone from C_9 to C_{13} forms a five-atom segment of a six-membered ring. The methyl substituents at C_9 and C_{13} form the sixth member of the ring. They are forced out of the plane yielding a curl-shaped structure. The C_{11}=C_{12} double bond becomes twisted with a torsion angle of −26° and the torsion angle of the C_{10}–C_{11} bond is −33°. The obtained structure is a local minimum on the ground-state potential energy surface. The two methyl groups on the retinyl chain prevent the completion of the rotation and in the opposite direction the twist is hindered by the torsion barrier of the C_{10}–C_{11} bond.

In this work, we discuss the obtained molecular structure of the curl-shaped retinal PSB isomer. Spectroscopic properties of the new retinal PSB isomer are compared to those obtained for the 11-*cis* and all-*trans* retinal PSBs. The calculated spectra might be used in future experimental characterization of the retinal PSB isomers. The calculations show that CD spectroscopy measurements detecting the differential absorption of left and right polarized light could be used to distinguish between the retinal PSB structures. Infrared (IR) spectra and nuclear magnetic resonance (NMR) shielding constants for the retinal PSB isomers are also reported.

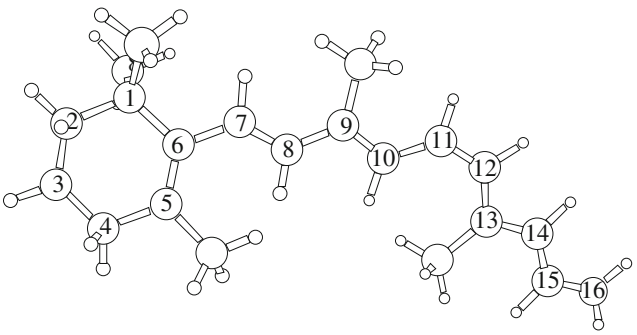

Fig. 1 The numbering of the carbon skeleton of the retinal PSB chromophores is shown

Computational methods

The molecular structures of the 11-*cis*, all-*trans*, and the curl-shaped retinal PSB isomers were optimized at the second-order Møller-Plesset perturbation theory (MP2) level using the Karlsruhe triple-ζ quality basis sets augmented with two sets of polarization functions (def2-TZVPP) [12] employing the resolution of the identity (RI) approach [13, 14]. The lowest excitation energies were calculated at the coupled-cluster approximate singles and doubles (CC2) level employing the RI approach [14–17]. In the CC2 calculations, the def2-TZVP basis set was used [12]. The def2-TZVP and def2-TZVPP basis sets are identical for C and N, whereas def2-TZVP has one *p* and *d* function less in the H basis set.

The molecular structures were also optimized at the density functional theory (DFT) level employing Becke's three parameter functional [18] in combination with the Lee-Yang-Parr correlation functional [19] (B3LYP) using the def2-TZVP basis set. The molecular structures were confirmed to be energy minima by calculating the harmonic vibrational frequencies using finite differences as implemented in the NUMFORCE program. The 6-s-*cis*(+) and 6-s-*cis*(−) retinal PSB isomers were also studied at the B3LYP level. The notation (+) and (−) indicates the sign of the torsion angle at the β-ionone ring. The optimized structures are given as supplementary material.

The electronic excitation spectra of the 11-*cis*, all-*trans*, and curl-shaped retinal PSB isomers were calculated at the time-dependent density functional theory (TDDFT) level [20–22] employing the B3LYP functional and the def2-TZVP basis sets. The rotatory strengths for the visible (Vis) and near-ultraviolet (UV) part of the electronic excitation spectrum of the retinal PSBs were calculated at the B3LYP TDDFT level. The optical activity measured in the circular dichroism (CD) experiments is related to the rotatory strength obtained in TDDFT calculations [23–27]. The rotatory strength is defined as the imaginary part of the scalar product between the electric and magnetic transition-moment vectors

$$R_{if} = \left|\vec{\mu}_{if}\right|\left|\vec{m}_{if}\right| \cos\left(\phi_{\vec{\mu}_{if},\vec{m}_{if}}\right) \quad (1)$$

where $\vec{m}_{if}$ is the magnetic transition moment calculated in the momentum representation so that R_{if} becomes origin independent [25, 26]. The magnetic and electric transition dipole moments $\vec{\mu}_{if}$ are given by

$$\vec{m}_{if} = \frac{e\hbar}{2mc}\int \Psi_i^* \vec{r} \times \vec{\nabla}\Psi_f d\vec{r}; \qquad \vec{\mu}_{if} = e\int \Psi_i^* \vec{r}\Psi_f d\vec{r}. \tag{2}$$

$\phi_{\vec{\mu}_{if},\vec{m}_{if}}$ is the angle between the transition dipole moments. The measured intensity difference $\Delta\epsilon$ (in dm^3 mol^{-1} cm^{-1}) is related to the rotatory strength (in cgs units) by

$$R_{if}^{\exp} = 2.297 \times 10^{-39}\int \frac{\Delta\epsilon}{\upsilon} d\upsilon\,. \tag{3}$$

Nuclear magnetic shielding constants which can be used to simulate the main features of the nuclear magnetic resonance (NMR) spectra of the retinal PSBs were calculated at the B3LYP level using the def2-TZVPP basis set [28–30]. All calculations have been done with the TURBOMOLE program package [31].

Results and discussion

Structures

The potential energy curve for the torsional twist motion of the β-ionone ring around the C_6–C_7 single bond shows that 11-*cis* retinal PSB has three stable isomers depending on the orientation of the β-ionone ring. In rhodopsin, 11-*cis* retinal has the 6-s-*cis*(−) structure with a β-ionone twist angle of about −40° [32]. The present B3LYP calculations on a single retinal PSB molecule show that the 6-s-*trans* structure with a torsion angle of 168° is the energetically lowest structure of the three 11-*cis* retinal PSB isomers distinguished by the orientation of the β-ionone ring. The second minimum at −39° corresponds to the conformation in the rhodopsin binding pocket. The third minimum in Fig. 2 corresponds to a 6-s-*cis*(+) structure with a torsion angle at the β-ionone ring of +32°. The two 6-s-*cis* structures differ from each other by having the methyl groups of the β-ionone ring tilted towards opposite sides of the retinyl chain plane. Depending on the direction, the potential barrier between the two 6-s-*cis* structures is 3–5 kJ/mol at the B3LYP level. The barrier height is large enough to prevent a thermal change of the conformation, because the barriers are often underestimated at the DFT level [33]. At the MP2 level, the obtained torsion barrier from the 6-s-*cis*(−) to the 6-s-*cis*(+) orientation is about 7 kJ/mol. The small energy barrier is due to the repulsion of

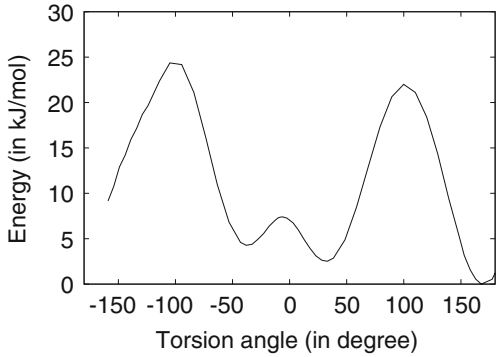

Fig. 2 The potential energy surface for 11-*cis* retinal PSB calculated at the B3LYP level for the torsion barrier of the β-ionone ring. All internal coordinates except the β-ionone ring torsion angle were optimized

the methyl groups at C_1 and C_5 and the hydrogens at C_7 and C_8 on the retinyl chain. According to the B3LYP frequency calculations the three isomers are minima on the ground-state potential energy surface.

Photoabsorption of the 11-*cis* retinal PSB leads to an isomerization reaction producing the all-*trans* isomer. The all-*trans* structure can analogously have the β-ionone ring in the three positions, because the coupling between the orientation of the β-ionone ring and the *cis* and *trans* structure of the C_{11}=C_{12} double bond is weak. In the gas phase, the 11-*cis* and all-*trans* isomers have an almost planar conformation of the retinyl chain. In rhodopsin, the retinyl chain is slightly distorted but still largely planar [8]. The 11-*cis* and all-*trans* isomers are depicted in Fig. 3a and b. Other obvious retinal PSB isomers can be constructed by permuting *cis* and *trans* orientations of the retinyl double bonds and the tilting angle of the β-ionone ring. To our knowledge, no other ground-state structures of the retinal PSB chromophores have been reported.

Here, we present calculations on a new isomer of the retinal PSB chromophore. The isomer has a strongly twisted retinyl chain with torsion angles significantly deviating from ±180° (0°) in the vicinity of the C_{11}=C_{12} double bond where the isomerization occurs. The largest structural differences appear for the C_9=C_{10}–C_{11}=C_{12} and C_{10}–C_{11}=C_{12}–C_{13} torsion angles. The angles are −33° and −26°, respectively, which can be compared to 178° and −2° for the 11-*cis* structure. For the all-*trans* retinal PSB, the corresponding angles are 180° and −179° at the B3LYP level. The structure is an intermediate between the *cis* and *trans* isomers but closer to *cis*. At the β-ionone ring and in the vicinity of the Schiff base, the retinyl chain of all studied retinal PSBs is more or less planar. The curl-shaped retinal PSB might therefore have energy minima for the three orientations of the β-ionone ring. The curl-shaped retinal PSB isomer is shown in Fig. 3c.

The graphs in Fig. 4 show that the curl-shaped retinal PSB has a slightly larger bond-length alternation than the

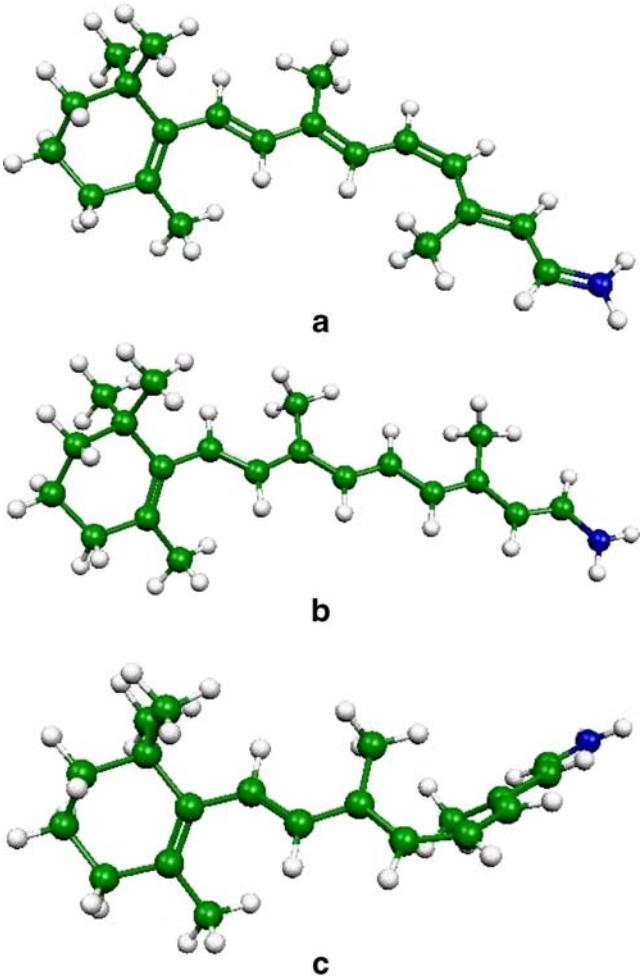

Fig. 3 The molecular structure of (**a**) the 11-*cis*, (**b**) all-*trans*, and (**c**) the curl-shaped retinal PSB chromophores calculated at the B3LYP level

11-*cis* and all-*trans* retinal PSBs. The bond-length alternation pattern for the curl-shaped isomer is more reminiscent of the bond-alternation pattern obtained for the all-*trans* retinal PSB than for the 11-*cis* retinal PSB. The largest difference appears for the C_{13}=C_{14} bond which is formally a double bond even though it is somewhat longer than the C_{12}–C_{13} single bond at the B3LYP level. At the MP2 level, the C_{13}=C_{14} double bond is 1.3 pm shorter than the C_{12}–C_{13} single bond. The C_{14}–C_{15} single bond is the second shortest carbon-carbon distance in the retinyl chain.

Because the curl-shaped molecule is slightly bent as compared to the 11-*cis* and all-*trans* isomers, its dipole moment of 12.7 D is somewhat smaller than the 13.9 D and 15.2 D obtained at the B3LYP level for the 11-*cis* and all-*trans* isomers, respectively. The Cartesian coordinates of the retinal PSB isomers are given as supporting information.

The methyl groups on the β-ionone ring interact with the retinyl chain resulting in local minima for three orientations of the ring. Experimentally, it has been found that the methyl groups play a role in the rhodopsin pigment formation [32]. For the pigment formation, the two methyl groups at C_1 are more important than the methyl group at C_5. The methyl groups at C_1 have previously been found to participate actively in the Franck-Condon relaxation of the first excited state; one of the C_1-Me bonds shrinks from 157 to 154.5 pm upon excitation [34]. The methyl groups on the retinyl chain also affect the quantum yield of the photo-isomerization reaction [35, 36]. The slower isomerization reaction of the 13-demethyl 11-*cis* retinal PSB has been suggested to be a consequence of missing steric interactions between the methyl group at C_{13} and the hydrogen at C_{10} [36]. The quantum yield is not much smaller for the isomerization reaction in hexane [37], whereas in rhodopsin the reaction efficiency is significantly affected by the methyl group. Thus, the methyl groups are thought to project the excited-state dynamics along the reaction pathway of the rhodopsin isomerization reaction [36]. The present study suggests a slightly different interpretation of the experimental observations. Assuming that the twisted retinal structure plays a role in the photo-isomerization reaction, the increased efficiency observed in the rhodopsin isomerization reaction might be due to steric interactions of the methyl groups at C_9 and C_{13}. The methyl-methyl repulsion interaction causes a strain in the retinyl chain at the isomerization centre. The strain is directed towards the C_{11}=C_{12} bond resulting in a twist of the bond and leading ultimately to the *cis-trans* isomerization reaction.

IR spectra

The vibrational frequencies were calculated for the optimized B3LYP structures using finite differences. The structures of the three retinal PSB isomers were found to be local minima with only real vibrational frequencies. The infrared (IR) spectra for the 11-*cis*, all-*trans*, and the curl-shaped retinal PSB isomers shown in Figs. 5, 6, and 7 were constructed from the B3LYP vibrational frequencies by using Lorentzian shape functions with a full width of half maximum (FWHM) of 5 cm^{-1} for the transitions. Unfortunately, it is not easy to assign all calculated frequencies to the corresponding signals in the experimental spectrum, but some of the bands can indeed be helpful for characterizing the isomers.

In the calculated spectra, the vibrational bands at 1600–1700 cm^{-1} corresponding to C–C stretching motions of the retinyl chain show distinct differences. This region of the IR spectrum might be useful for detecting the isomers in the sample. Significant differences are also seen in the C–C fingerprint region at about 1200 cm^{-1}. The calculated vibration spectra in the C–C fingerprint region seem to be blue shifted by about 30 cm^{-1} as compared to the experimental one. Experimentally, the three strong bands for 11-*cis* retinal PSB in the fingerprint region appear at

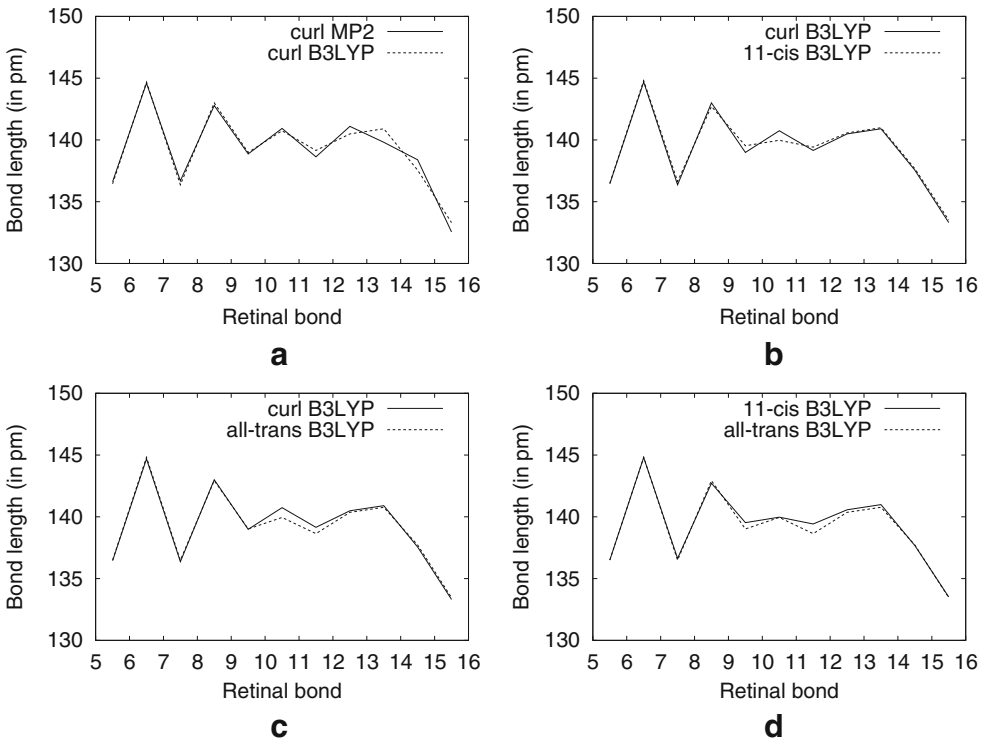

Fig. 4 Comparison of the bond-length alternation of the studied retinal PSB isomers. The bond-length alternation of the curl-shaped isomer calculated at the MP2 and B3LYP level are compared in (**a**). In (**b**), (**c**), and (**d**) the bond-length alternation of the 11-*cis*, all-*trans*, and the curl-shaped isomers calculated at the B3LYP level is compared. The bond length is given between the integers labeling the corresponding carbon atoms

1214, 1238, and 1268 cm^{-1} [36], whereas the computed spectrum shows the three strongest transitions at 1254, 1268, and 1300 cm^{-1}. The most intense peak in the experimental IR spectrum of 11-*cis* retinal PSB appears at 1548 cm^{-1} as compared to the value of 1543 cm^{-1} calculated at the B3LYP level. The peaks in the hydrogen-out-of-plane (HOOP) region of the vibrational spectra at 900–1000 cm^{-1} have low intensities. For 11-*cis* retinal PSB, the first strong peak in the HOOP region appears at 970 cm^{-1} in the experimental spectrum as compared to 989 cm^{-1} obtained at the B3LYP level. To draw a distinction between the isomers based on the HOOP frequencies is thus difficult even though the peak patterns slightly differ.

UV-Vis spectra

In a recent study, we found that the lowest excitation energy of 11-*cis* retinal PSB at the B3LYP level is about 0.3 eV larger than obtained experimentally [38]. The second excitation energy calculated at the B3LYP level is 0.12 eV smaller than the experimental value [39]. Coupled-cluster approximate singles and doubles (CC2) calculations yielded more accurate excitation energies. At the CC2 level, the

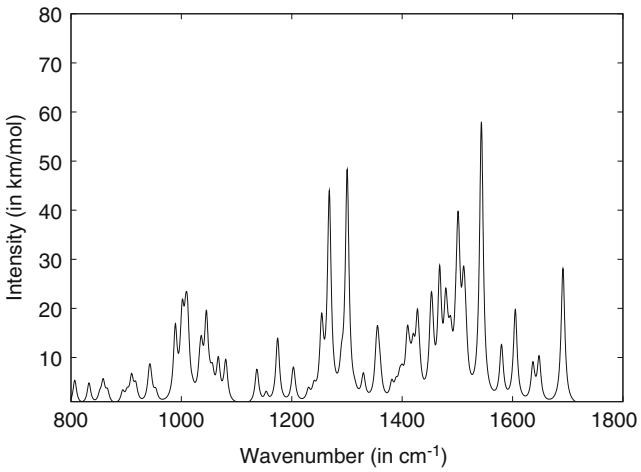

Fig. 5 The IR spectrum of the 11-*cis* retinal PSB calculated at the B3LYP DFT level

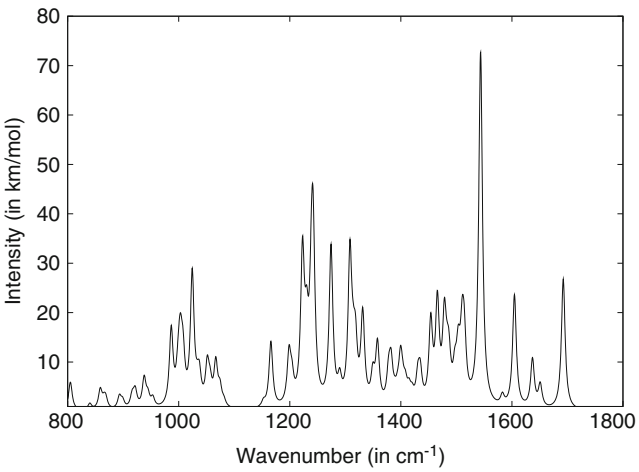

Fig. 6 The IR spectrum of the all-*trans* retinal PSB calculated at the B3LYP DFT level

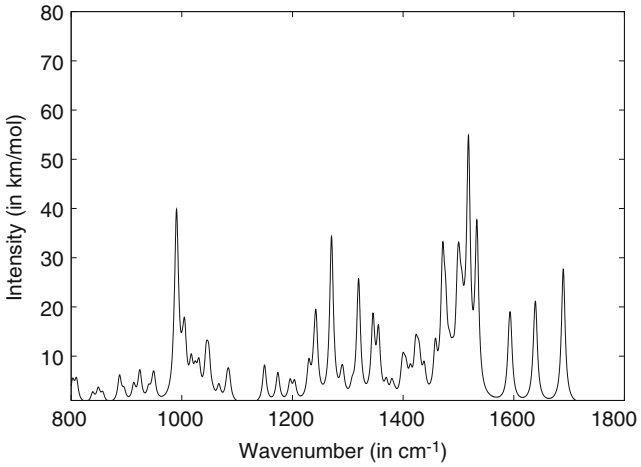

Fig. 7 The IR spectrum of the curl-shaped retinal PSB calculated at the B3LYP DFT level

two first excitation energies of 2.136 eV and 3.206 eV for 11-*cis* retinal PSB agreed within 0.1 eV with the experimental values measured in the gas phase [38, 39]. For the curl-shaped isomer the corresponding excitation energies are 2.029 eV and 3.180 eV as compared to the B3LYP values of 2.221 eV and 3.020 eV.

The CC2 excitation energies for the retinal chromophore are more accurate than the values recently obtained in calculations at the complete active space self-consistent field (CASSCF) level in combination with second-order perturbation theory corrections (CASPT2) [40–42]. A comparison of the B3LYP and CC2 excitation energies for the third to fifth excited states of 11-*cis* retinal PSB shows that the B3LYP excitation energies for these states are 0.35-0.53 eV smaller than the CC2 ones [11, 34]. The electronic excitation spectra up to 6 eV were calculated for the retinal PSB isomers at the B3LYP level using the TZVP basis set. The B3LYP excitation energies of the three retinal PSB isomers are given in Table 1. The lowest excitation energies are 0.1 eV smaller for the curl-shaped isomer than for 11-*cis* retinal PSB. The uncertainty in the transition energies for the higher excited states of the retinal PSB isomers are significantly larger than 0.1 eV. As shown for the CD-spectra below, the relative positions of the excitation energies can in principle be useful for an identification of the retinal PSB isomers. However, the energy differences between transitions might be too small to distinguish between them experimentally.

CD spectra

Circular dichroism (CD) spectroscopy detects the differential absorption of left and right polarized light. It is an important tool for determining the absolute configuration of optically active molecules [24–27, 43, 44]. For comparison with experiment, the spectra have been modelled with

Table 1 The first few excitation energies (in eV) of the retinal PSB isomers calculated at the B3LYP/def2-TZVP level

State	11-*cis*	all-*trans*	curl-shaped
2A	2.342	2.340	2.221
3A	3.103	3.133	3.020
4A	3.745	3.728	3.647
5A	3.869	3.897	3.747
6A	4.111	4.110	4.025
7A	4.287	4.278	4.161
8A	4.392	4.426	4.245
9A	4.889	4.852	4.742
10A	4.914	4.959	4.784
11A	5.011	4.983	4.933
12A	5.170	5.145	5.097
13A	5.211	5.194	5.133
14A	5.338	5.417	5.245
15A	5.449	5.486	5.309
16A	5.479	5.501	5.447
17A	5.561	5.678	5.482
18A	5.626	5.698	5.506
19A	5.675	5.730	5.623
20A	5.810	5.782	5.671
21A	5.820	5.861	5.746
22A	5.867	5.887	5.767
23A	5.906	5.991	5.860
24A	5.958	6.018	5.927
25A	5.982	6.062	5.960

Gaussian line shapes having a root mean square width of 0.1 eV. The CD spectra calculated for the 11-*cis*, all-*trans*, and the curl-shaped retinal PSBs are shown in Figs. 8, 9, and 10. In the CD spectrum of the 11-*cis* retinal PSB, all the transitions in the visible and near UV part of the electronic excitation spectrum have positive intensities. For the all-*trans* retinal PSB, the first transition has a strong positive intensity, whereas the weaker peaks between 300 nm and 400 nm have negative intensities in the CD

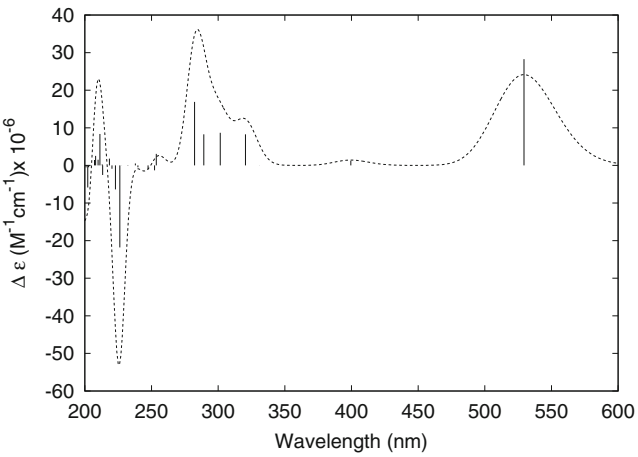

Fig. 8 The CD spectrum of the 11-*cis* retinal PSB calculated at the B3LYP TDDFT level. The β-ionone ring torsion angle is −39°

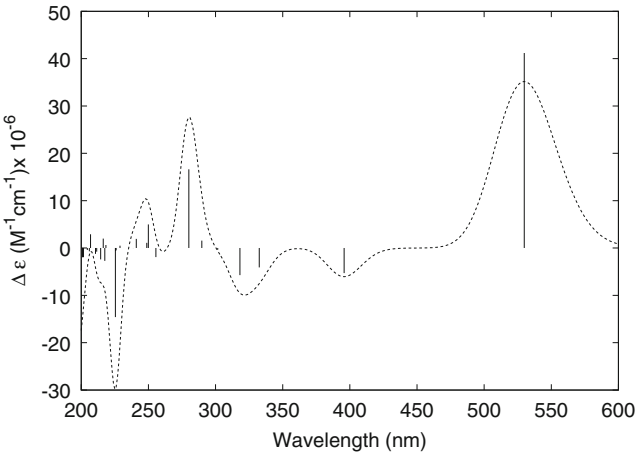

Fig. 9 The CD spectrum of the all-*trans* 6-s-*cis*(−) retinal PSB calculated at the B3LYP TDDFT level. The β-ionone ring torsion angle is −37°. The CD spectrum of the all-*trans* 6-s-*cis*(+) retinal PSB differs from that of all-*trans* 6-s-*cis*(−) retinal PSB by having an opposite sign for all the peaks shown in the graph

spectrum. For the curl-shaped isomer, the first strong transition has a positive intensity and it is slightly redshifted as compared to the two other isomers. The electronic transitions above 250 nm are very weak as compared to the corresponding peaks for the 11-*cis* and all-*trans* isomers. The weak transitions in the CD spectrum of the curl-shaped retinal PSB have negative intensities. The CD spectra calculated for the 11-*cis*, all-*trans*, and the curl-shaped retinal PSB isomers thus differ significantly. CD spectroscopy can most likely be used to identify the retinal PSB isomers.

The potential energy curve for the torsion twist of the β-ionone ring of the 11-*cis* retinal PSB shown in Fig. 2 has three minima. As discussed above, two of the minima correspond to 6-s-*cis* structures. The calculated CD spectra for the two 6-s-*cis* configurations are shown in Figs. 8 and 11. The CD spectrum of the 6-s-*trans* conformer is shown

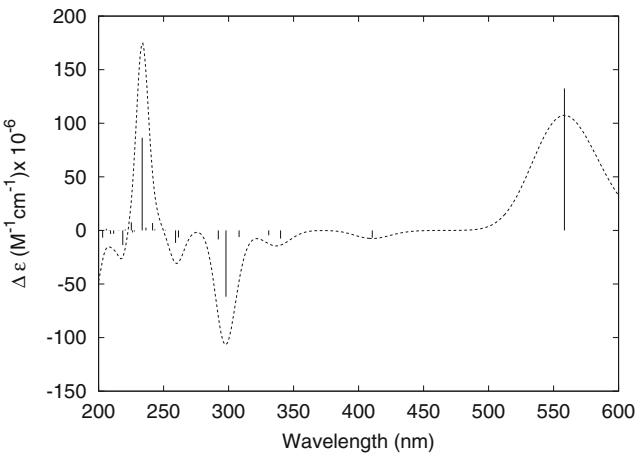

Fig. 10 The CD spectrum of the curl-shaped retinal PSB calculated at the B3LYP TDDFT level. The β-ionone ring torsion angle is −36°

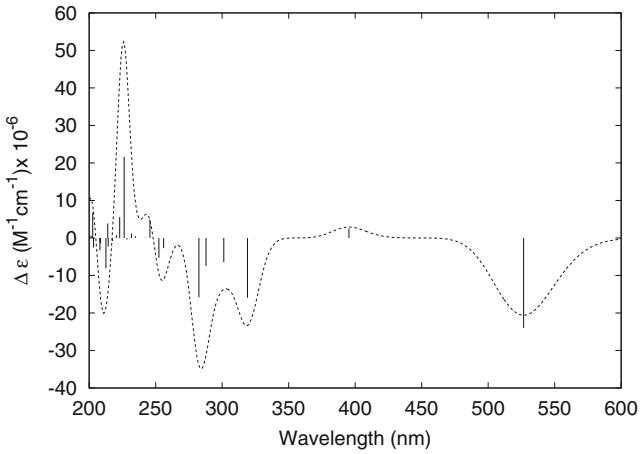

Fig. 11 The CD spectrum of the 11-*cis* retinal PSB calculated at the B3LYP TDDFT level. The β-ionone ring torsion angle is +32°

in Fig. 12. The difference to the spectra of the 6-s-*cis* conformers is obvious by the change of sign between the strong peaks around 500 and 300 nm. Even though it is difficult to visually discover the structural difference between the two 6-s-*cis* retinal PSB isomers with +32° and −39° orientations of the β-ionone ring, the CD spectra are completely different. The sign of the torsion angle of the β-ionone ring could be determined using CD spectroscopy. The CD spectrum measured for rhodopsin displays two positive peaks at 500 nm and 335 nm, respectively [45, 46]. For bathorhodopsin, the first peak is slightly redshifted as compared to rhodopsin. In addition, the first peak in the CD spectrum of bathorhodopsin has a negative intensity [45, 46]. The change in the sign of the intensity of the first peak suggests that bathorhodopsin and rhodopsin have different orientations of the β-ionone ring, namely that the primary photoreaction step during the first 1 ps involves a flip of the β-ionone ring from the 6-s-*cis*(−) to a 6-s-*cis*(+) orientation. This does not necessarily involve a movement

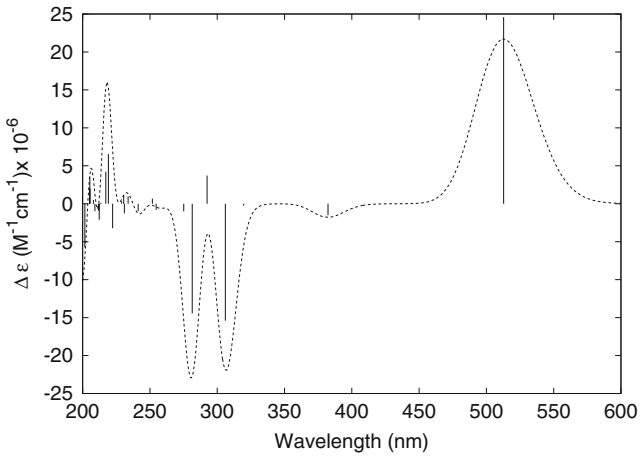

Fig. 12 The CD spectrum of 11-*cis* retinal PSB calculated at the B3LYP TDDFT level. The β-ionone ring torsion angle is 168°

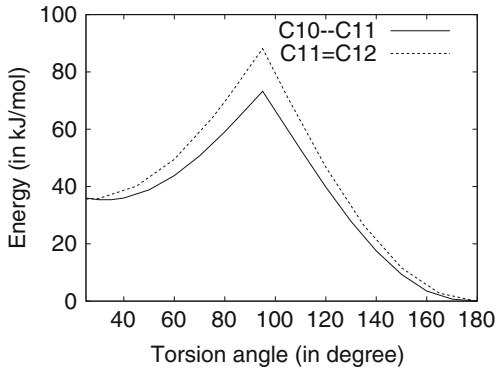

Fig. 13 The ground-state torsion barriers (in kJ/mol) for the twist of the C_{10}–C_{11} single bond and the C_{11}=C_{12} double bond of the curl-shaped retinal PSB calculated at the B3LYP level. The curl-shaped isomer corresponds to the minimum at −33° along the C_{10}–C_{11} twisting coordinate and to the minimum at −26° along the C_{11}=C_{12} twisting coordinate. The minimum at −180° corresponds to 11-*cis* retinal PSB for the C_{10}–C_{11} bond twist and to the 10-s-cis isomer of all-*trans* retinal PSB for the C_{11}=C_{12} bond twist. The potential energy curves are adjusted to have the same energy at the minimum. Calculations have been performed by optimizing all internal coordinates except the twisting angle

of the ring moiety relative to the protein-cavity. The β-ionone ring has been subject of experimental studies that have focussed on distinguishing a 6-s-*cis* from a 6-s-*trans* conformation. To our knowledge, a possible change from a 6-s-*cis*(−) to a 6-s-*cis*(+) orientation has not been discussed [47]. A comparison of the X-ray structures for rhodopsin and bathorhodopsin reveals some structural changes also at the β-ionone ring [8]. Our calculations of the CD spectra using the rhodopsin and bathorhodopsin structures optimized in the binding pocket as well as similar calculations by Schreiber et al. [9] using the same structure show that the surrounding protein also affects the CD spectra making the CD spectrum of 6-s-*cis*(−) bathorhodopsin embedded in the protein more reminiscent of the recorded one.

NMR spectra

The isotropic nuclear magnetic shielding constants were calculated for the three retinal PSB isomers at the B3LYP level. The obtained ^{1}H and ^{13}C shielding constants are very similar. Nuclear magnetic resonance (NMR) spectroscopy is probably not very helpful to distinguish between the isomers. The largest differences in the ^{13}C magnetic shielding shifts compared to the 11-*cis* and all-*trans* retinal PSBs occur at the isomerization centre where the curl-shaped isomer is twisted. For C_{11} and C_{12}, the ^{13}C NMR shieldings of the curl-shaped isomer differ by 6 ppm as compared to the 11-*cis* retinal PSB. The ^{13}C NMR shieldings calculated for the all-*trans* retinal PSB are closer to those obtained for the curl-shaped isomer, except for C_{11} where the ^{13}C NMR shieldings differ by 6 ppm. The NMR chemical shifts obtained using the calculated magnetic shieldings for the retinal PSB isomers and for the tetra methyl silane (TMS) reference substance can be compared to experimental values. The calculated isotropic shielding constants for TMS, 11-*cis*, all-*trans*, and the curl-shaped retinal PSBs are given as supplementary material.

Potential energy curves

The molecular structure of the curl-shaped retinal PSB was obtained by optimizing its ground-state structure using a start geometry taken from an excited-state optimization of the 11-*cis* retinal PSB structure [11]. The curl-shaped isomer has a twisted structure in the vicinity of the C_{11}=C_{12} double bond where 11-*cis* to all-*trans* retinal PSB photo isomerization occurs. The twisted configuration is a trapped structure between the 11-*cis* and all-*trans* structures. The structure of the curl-shaped isomer is stabilized by steric interactions of the two methyl groups on the retinyl chain and rotation around the C_{10}–C_{11} single bond towards the 11-*cis* structure is prevented by a barrier. The steric repulsion between the methyl groups directs the torsion strain towards the C_{11}=C_{12} double bond. The torsion barriers for the C_{10}–C_{11} single-bond and C_{11}=C_{12} double-bond twists calculated at the B3LYP level are 38 kJ/mol and 52 kJ/mol, respectively. The potential energy curves for the bond twists are shown in Fig. 13. They were obtained at the B3LYP level by optimizing all internal coordinates except the twisting coordinate. Difficulties of the B3LYP method to describe states with pronounced multireference character result in cusps of the potential energy curves in Fig. 13.

The torsion barriers of the C_{10}–C_{11} single bond calculated for the ground and first excited state are compared in Fig. 14. The ground-state potential curve was obtained at the MP2 level and for the first excited state it was calculated at the CC2 level. The graph shows that the

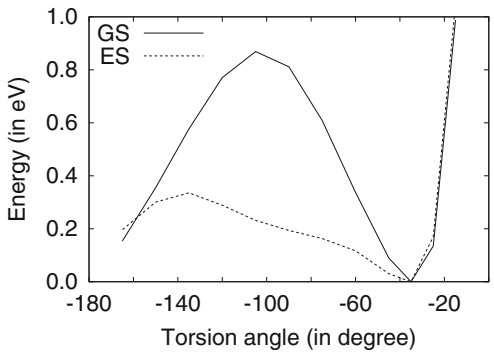

Fig. 14 The torsion barriers (in eV) for the torsion twist of the C_{10}–C_{11} single bond calculated at the MP2 level for the ground state (GS) and at the CC2 level for the first excited state (ES). The potential energy curves are adjusted to have the same energy at the minimum. The curl-shaped and the 11-*cis* isomers correspond to the minima at −34° and −180°, respectively

minimum corresponding to the curl-shaped configuration at −34° is separated from the 11-*cis* structure by a barrier of 84 kJ/mol at the MP2 level. For the first excited state, the CC2 torsion barrier is 32 kJ/mol which is more than a factor of three smaller than for the ground state. The actual torsion barriers at MP2 and CC2 level are smaller because the rest of the internal coordinates has been kept fixed in the single-point calculations of the potential energy curves. The frozen internal coordinates were adopted from the optimized ground-state structure of the curl-shaped retinal PSB. The torsion barriers calculated at MP2 and CC2 level cannot directly be compared to the torsion barriers obtained at the B3LYP level. In the DFT calculations, all internal coordinates except the twisting coordinate were fully optimized. Since the MP2 and CC2 torsion barriers refer to single-point calculations it is natural that the barriers are much higher than those obtained in the B3LYP optimizations.

Conclusions

The molecular structures and spectroscopic properties of the 11-*cis*, all-*trans*, and a curl-shaped retinal PSB have been studied at B3LYP DFT and ab initio MP2 and CC2 levels. The computational study shows that the retinal PSB chromophore has a low-lying isomer with a twisted retinyl chain. The torsion angles of the C_{10}–C_{11} and C_{11}=C_{12} bonds are −33° (−34°) and −26° (−24°) at the B3LYP level. At the B3LYP level, the new isomer lies only 35 kJ/mol (22 kJ/mol) above the 11-*cis* structure. The corresponding MP2 values are given within parenthesis. The calculations also show that retinal PSBs have local minima on the potential energy surface for three orientations of the β-ionone ring. Two of them have 6-s-*cis* conformation with the methyl groups tilted towards opposite sides of the retinyl chain plane. The third minimum has a 6-s-*trans* orientation of the β-ionone ring. The calculated CD spectra are qualitatively different suggesting that the sign of the torsion angle of the β-ionone ring might be obtained using CD spectroscopy. Comparison of calculated and measured CD spectra for rhodopsin and bathorhodopsin suggests a flip of the β-ionone ring during the first 1 ps of the photoreaction. The orientation of the β-ionone ring for rhodopsin is 6-s-*cis*(−), whereas bathorhodopsin seems to have a 6-s-*cis*(+) conformation. However, the surrounding protein significantly affects the CD spectra making the CD spectrum of 6-s-*cis*(−) bathorhodopsin more reminiscent of the recorded CD spectrum of bathorhodopsin. The calculated IR and CD spectra for the curl-shaped retinal PSB differ from those obtained for 11-*cis* retinal PSB. Significant differences in the IR spectra are obtained for the vibrational bands in the C–C stretching region and for the fingerprint bands. Thus, the curl-shaped retinal PSB isomer might be identified using IR and CD spectroscopy, whereas the NMR and UV-Vis spectra might be less helpful for that purpose. The largest difference in the ^{13}C NMR chemical shift is 6 ppm obtained for the C_{11} and C_{12} carbons. The difference in the electronic excitation energies are less than 0.2 eV for all states considered in the calculations.

The calculations also suggest that retinal PSB structures reminiscent of the curl-shaped isomer might play an important role for the photo-isomerization reaction. For the curl-shaped isomer, the torsion twist in the direction towards the all-*trans* isomer is prevented by the steric interaction between the two methyl groups on the retinyl chain. One can speculate that one reason for the presence of the methyl groups on the retinyl chain is that their positions are optimal for the isomerization to occur at the C_{11}=C_{12} double bond and not at the other double bonds of the retinyl chain.

Acknowledgements This research has been supported by the Academy of Finland through its Centers of Excellence Programme 2006–2011 and the OPNA research project (118195). We also thank CSC - the Finnish IT Center for Science for computer time. This work was also supported by the Center for Functional Nanostructures CFN of the Deutsche Forschungsgemeinschaft DFG within Project C3.9.

References

1. Shichida Y, Kobayashi T, Ohtani T, Yoshizawa T, Nakakura S (1978) Photochem Photobiol 27:335–341
2. Yoshizawa T, Shichida Y, Matuoka S (1984) Vision Res 24:1455–1463
3. Shichida Y, Matuoka S, Yoshizawa T (1984) Photobiochem Photobiophys 7:221–228
4. Schoenlein RW, Peteanu LA, Mathies RA, Shank CV (1991) Science 254:412–415
5. Kandori H, Shichida Y, Yoshizawa T (2001) Biochemistry (Moscow) 66:1197–1209
6. Kukura P, McCamant DW, Yoon S, Wandschneider DB, Mathies RA (2005) Science 310:1006–1009
7. Okada T, Ernst OP, Palczewski K, Hoffmann KP (2001) Trends Biochem Sci 26:2759–2767
8. Nakamichi H, Okada T (2006) Angew Chem Int Ed 45:4270–4273
9. Schreiber M, Sugihara M, Okada T, Buss V (2006) Angew Chem Int Ed 45:4274–4277
10. Yoshizawa T, Wald G (1963) Nature 197:1267–1286
11. Send R, Sundholm D (2007) J Phys Chem A 111:8766–8773
12. Weigend F (2006) Phys Chem Chem Phys 8:1057–1065
13. Weigend F, Häser M (1997) Theoret Chem Acc 97:331–340
14. Hättig C, Weigend F (2000) J Chem Phys 113:5154–5161
15. Christiansen O, Koch H, Jørgensen P (1995) Chem Phys Lett 243:409–418
16. Köhn A, Hättig C (2004) J Am Chem Soc 126:7399–7410
17. Hättig C (2005) Adv Quantum Chem 50:37–60
18. Becke AD (1993) J Chem Phys 98:5648–5652
19. Lee C, Yang W, Parr RG (1988) Phys Rev B 37:785–789
20. Bauernschmitt R, Ahlrichs R (1996) Chem Phys Lett 256:454–464
21. Furche F, Ahlrichs R (2002) J Chem Phys 117:7433–7447

22. Furche F, Ahlrichs R (2004) J Chem Phys 121:12772–12773
23. Bour P (1999) J Phys Chem A 103:5099–5104
24. Furche F, Ahlrichs R, Wachsmann C, Weber E, Sobanski A, Vögtle F, Grimme S (2000) J Am Chem Soc 122:1717
25. Grimme S, Furche F, Ahlrichs R (2002) Chem Phys Lett 361:321
26. Autschbach J, Ziegler T, van Gisbergen SJA, Baerends EJ (2002) J Chem Phys 116:6930
27. Sundholm D (2003) Phys Chem Chem Phys 5:4265–4271
28. Häser M, Ahlrichs R, Baron HP, Weis P, Horn H (1992) Theoret Chim Acta 83:455
29. Kollwitz M, Gauss J (1996) Chem Phys Lett 260:639–646
30. Kollwitz M, Häser M, Gauss J (1998) J Chem Phys 108:8295–8301
31. Ahlrichs R, Bär M, Häser M, Horn H, Kölmel C (1989) Chem Phys Lett 162:165–169
32. Domínguez M, Álvarez R, Pérez M, Palczewski K, de Lera AR (2006) ChemBioChem 7:1815–1825
33. Sundholm D, Konschin H, Häser M (1999) Chem Eur J 5:267–273
34. Send R, Sundholm D (2007) J Phys Chem A 111:27–33
35. Schoenlein RW, Peteanu LA, Wang Q, Mathies RA, Shank CV (1993) J Phys Chem 97:12087–12092
36. Lin SW, Groesbeek M, van der Hoef I, Verdegem P, Lugtenburg J, Mathies RA (1998) J Phys Chem B 102:2787–2806
37. Becker RS, Freedman K (1985) J Am Chem Soc 107:1477–1485
38. Send R, Sundholm D (2007) Phys Chem Chem Phys 9:2862–2867
39. Nielsen IB, Lammich L, Andersen LH (2006) Phys Rev Letters 96:018304
40. Cembran A, González-Luque R, Altoè P, Merchán M, Bernardi F, Olivucci M, Garavelli M (2005) J Phys Chem A 109:6597–6605
41. Cembran A, Bernardi F, Olivucci M, Garavelli M (2005) Proc Natl Acad Sci USA 102:6255–6260
42. Sekharan S, Weingart O, Buss V (2006) Biophys J 91:L07–L09
43. Stephens PJ, McCann DM, Devlin FJ, Cheeseman JR, Frisch MJ (2004) J Am Chem Soc 126:7514–7521
44. Pecul M, Ruud K, Helgaker T (2004) Chem Phys Letters 388:110–119
45. Shichida Y, Tokunaga F, Yoshizawa T (1978) Biochim Biophys Acta 504:413–430
46. Horiuchi S, Tokunaga F, Yoshizawa T (1980) Biochim Biophys Acta 591:445–457
47. Liu RSH, Hammond GS, Mirzadegan T (2005) Proc Natl Acad Sci 102:10783